International Journal of Scientific Research in Science and Technology
Print ISSN: 2395-6011 | Online ISSN: 2395-602X (www.ijsrst.com)
doi : https://doi.org/10.32628/IJSRST218511

# Structural and UV-Vis Diffuse Reflection Spectroscopy Studies of Nanosized $Sr_{0.5}Ba_{0.5}Nb_2O_6$ synthesized by Co-Precipitation method

**S. B. Nagdeote**
Department of Physics, Amolakchand Mahavidyalaya, Yavatmal, Maharashtra, India

**Article Info**
Volume 8, Issue 5
Page Number : 78-83

**Publication Issue**
September-October-2021

**Article History**
Accepted : 08 Sep 2021
Published : 15 Sep 2021

## ABSTRACT

The $Sr_{0.5}Ba_{0.5}Nb_2O_6$ (SBN-50) is Synthesis by coprecipitation method in nanoscale. TG/DTA shows the reaction and tetragonal phase formation occur at low temperatures, due to which the good homogeneity and morphology of the particles is observed. The average size of the particles was found to be ~ 45 nm. The lattice parameters is found very close to the reported values of single crystals despite method of synthesis and size of the particles. A reflectance spectrum in UV and visible regions shows less reflectance for 337nm and 519nm respectively.

**Keywords** : Nanoparticles, TG/DTA, FTIR, Reflectance spectra, XRD

## I. INTRODUCTION

Strontium barium niobates $Sr_xBa_{1-x}Nb_2O_6$ (SBN) is lead free functional material crystallizes in the tetragonal tungsten bronze (TTB) structure was first reported as ferromagnetic material in1960 by Francombe. Since then it was extensively studied for their good ferroelectric [1], electro-optic[2], photorefractive[3], pyroelectric and dielectric properties[4,5]. It is very attractive material for various applications particularly for light wave application and optical storage. It was also studied largely for transverse electro-optic effect. These properties can be enhance by varying the composition of Sr and Ba, as well as by doping various elements. The compositions of Sr and Ba is brought out various changes in the structural and show a wide variation of the non-equivalent crystallographic positions in its structure [6-8]. The photorefractive properties of SBN crystal was affected by doping with cerium and chromium (2,9). However, the particle size, sinterability and homogeneity of material are also important as it also affected on properties of SBN[10]. The particles sized of the materials are achieved by synthesis methods. [11, 12]
In the present research work, $Sr_{0.5}Ba_{0.5}Nb_2O_6$ (SBN-50) was synthesized by co-precipitation method successively. The DTA and TGA analysis indicate information about the crystalisation temperature of material. TEM and XRD studies conformed formation of material in nanoscale with particles sized 45nm.the material is characterized by XRD, FTIR spectroscopy and UV-vis diffused reflectance spectroscopy have been employed for studying the vibration information and band gap.

## II. EXPERIMENTAL

SBN-50 nanoparticles were synthesized by a simple coprecipitation (wet chemical) method as reported [13] with some modification. All the constituent chemicals used for the synthesis of SBN-50 nanoparticles were of AR grades. First, the stoichiometric amount of $Nb_2O_5$ was converted to transparent solution of $NbF_5$ by reacting $Nb_2O_5$ with minimum amount of HF in hot water bath for 24h.then (1:1) mixture solution of $SrCl_2$. $6H_2O$ and $BaCl_2.2H_2O$ was prepared by dissolving these chlorides into distilled water. These two solutions were added and mixed well by using a magnetic stirrer for 3-4 h. While stirring, an excess quantity of concentrated HCl was added to the above solution to dissolve the Barium fluoride and Strontium fluoride formed during the reactions of $NbF_5$ and $BaCl_2.2H_2O$ and $SrCl_2$. $6H_2O$. A mixture of ammonium oxalate and ammonium hydroxide in the ratio(25:75) was then added drop wise to precipitate barium and strontium as oxalates and niobium as hydroxide. During the entire reaction pH was maintained around 10. The precipitated obtained in the process was then filtered and washed several times with the distilled water. The washed powder was then dried at $70^0$C in oven for 24 hrs. The thermal decomposition and crystallization of the precursor were investigated by thermogravimetry and differential thermal analysis (TG-DTA, SHIMATZU, DTG-60) in static air with the heating rate of $5^0$C/min. The X-ray diffraction (XRD) data of the powder (calcined at $750^0$C for 6 hours) was recorded at room temperature by using X-ray diffractometer (D8 ADVANCE, Bruker, Germany) employing Cu Kα radiation with step size of $0.02^0$ and step time of 46.5 sec per degree. The crystallite size of the particles was estimated from the full width at half maximum by the Scherrer's equation. The morphology of the particles was analyzed by using transmission electron microscopy (TEM) (TECNAI G2 20 ULTRA-TWIN, FEL, Netharland).

For the study, pallets of $Sr_{0.5}Ba_{0.5}$ $Nb_2O_6$ were prepared. The calcined powder was mixed with few drops of 1 wt% solution of polyvinyl alcohol and isostatically pressed into pallets under pressure of 5-6 tons for 5 min. The pallets were then sintered at $700^0$C for 10 h. The surfaces of the sintered pallets were polished mechanically and coated with the silver paint. The UV-VIS reflectance spectrum of synthesized calcined particles is recorded by using SHIMATZU make UV-VIS spectrometer (UV-1700).

## III. Results and Discussion

### 3.1 TG/ DTA study

The TG/DTA curves of as synthesized precursor of SBN-50 are shown in Figure 1. These curves are different from the earlier reported nature using traditional sintering method [10,14]. The TGA curve shows the total weight loss of precursor precipitate is only 6.75%, confirms that the bi-products of the reaction were already removed from the precursor during the washing and drying process except the carbon monoxide gas, according to the reaction,

$$2Nb(OH)_5 + \tfrac{1}{2}\,Ba\,C_2O_4 + \tfrac{1}{2}\,Sr\,C_2O_4 \rightarrow Sr_{0.5}Ba_{0.5}Nb_2O_6.CO + 5H_2O + CO_2\uparrow$$

$$Sr_{0.5}Ba_{0.5}Nb_2O_6.CO \rightarrow Sr_{0.5}Ba_{0.5}Nb_2O_6 + CO\uparrow$$

Since oxalates of Sr and Ba are formed at initially stage, one of the bi-products is carbon monoxide which can be removed at higher temperature [14].

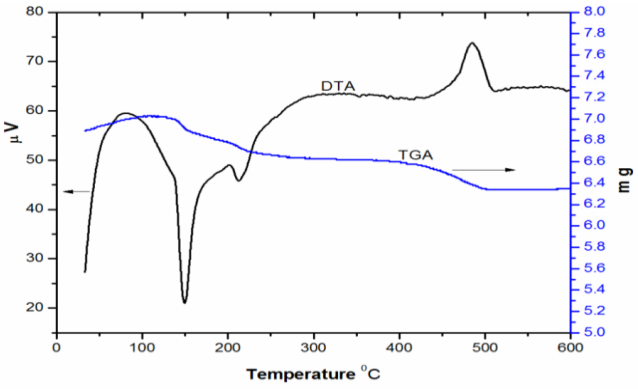


Figure 1 TG/DTA Curves of precursor of SBN-50 obtained by coprecipitation method.

The TGA curve, shows the initial region of weight gain which is due to the reaction of precursor with the air atmosphere. The broader exothermic peak is observed at 83$^0$C will be due to this effect. Mainly three regions of weight loss and corresponding DTA peaks, two endothermic effects and one exothermic are observed. The first endothermic peak is observed at 152$^0$C and the related weight loss, which was calculated from TG curve, is 1.715%. This can be assigned to the burn out of organic impurities and evaporation of moisture present in the precursor. The second endothermic peak is observed at 215.3$^0$C and the related weight loss shown by TG curve is about 2.4%. This decomposition is assigned to the removal of fraction of carbon monoxide. The third exothermic peak is observed at 487.6$^0$C and can be assigned to the phase change as well as simultaneous removal of remaining fraction of carbon monoxide. The loss of weight during the reaction is 3.13%. After 512$^0$C, no further changes in TG and DTA curves. For good crystallization the sample was calcined at temperature 750$^o$c.

### 3.2. Morphological and Structural

Figure 2 shows the refined pattern along with XRD patterns of SBN-50.The refinement of the XRD data was done by the Rietveld refinement method, FULLPROF. The goodness of fit (S) factor was found to be 1.5, shows good agreement of theoretical pattern with the experimentally observed pattern. The observed phase of the synthesized SBN-50 is tetragonal, space group is P4bm and the lattice parameters are: a = b = 12.4850Å and c = 3.9497Å. These values of lattice parameters are closer to the literature reported values (a = 12.461 Å and c= 3.9475 Å, [8]) of SBN-50 single crystals than the earlier reported one for nanoparticles by traditional sintering method [10], and coprecipitation method [13].

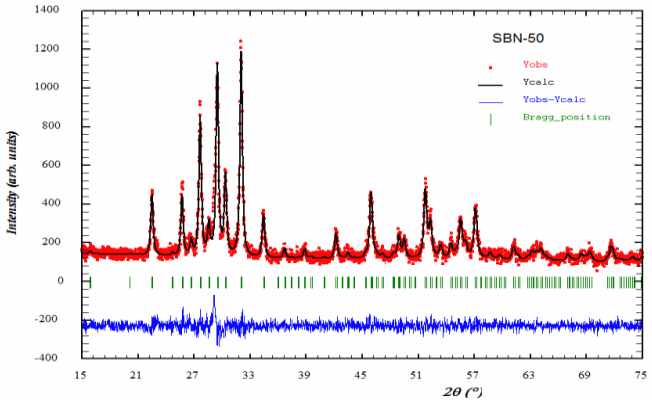


Figure 2 XRD patterns showing observed and calculated spectra of SBN-50 (using Rietveld refinement FULLPROF).

The size of the particles was calculated from the XRD pattern using Scherer's formula,

$$D = \frac{k\lambda}{\beta cos\theta}$$

where, D is the average grain size, assuming particles are spherical k is equal to 0.89, λ is the X-ray wavelength, θ is the peak angle, and $\beta$ is full width at half the maxima. The average grain size of the particles was found to be 30 nm.

### 3.3. FTIR spectra

The FTIR spectra of nanosized SBN in the range 400 to 4000 cm$^{-1}$ at room temperature as shown in the Fig3. From the spectra, It is observed that the strong band occur at wave numbers 646,1071, 1470, 1633, and 3413cm$^{-1}$. The band at wave numbers 645 cm$^{-1}$ is assigned to the Nb-O bond vibration, which is the characteristic bond of niobate groups. [15]. The peak at wave numbers 1071 cm$^{-1}$,which may be assigned to the asymmetric stretching of O-Ba (O-Sr). The observed band at 1470 and 1633, is the confirmation of the BO6 octahedral group of the material. The bands 3413 cm$^{-1}$ is attributed to the hydrogen bonds and due the stretching of OH$^-$ probably as a result of humid atmosphere or may be due to water molecules from the moisture [16].

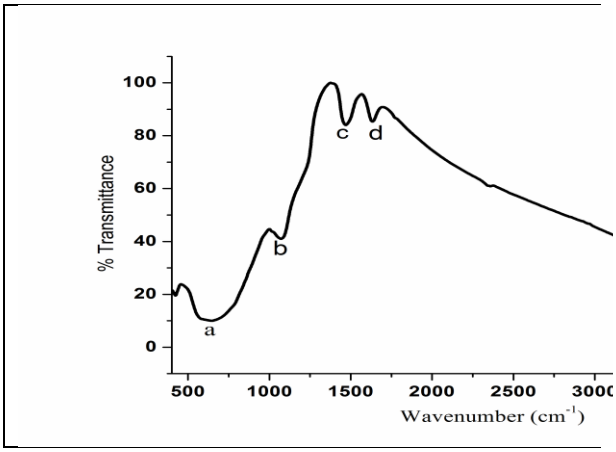


Figure 3: The FTIR spectra of SBN50 at room temperature

TEM and HRTEM images of synthesized SBN-50 are shown in Figures 4a and 4b respectively. Figure 4a shows that the particles are homogeneous, spherical and agglomerated; whereas Figure 4b shows the lattice fringes terminated at the well-defined grain boundary. The better homogeneity is due to the occurrence of crystallization at relatively low temperature. Figure 4c is the SAED image of synthesized SBN-50 materials. The white dots over rings are indicating well crystallization of the material at 750$^0$C. The average size of particles was estimated by taking the average of dimensions of 10 particles in the TEM image and it was found 45 nm. The discrepancy in the size could be attributed to the agglomeration of nanoparticles.

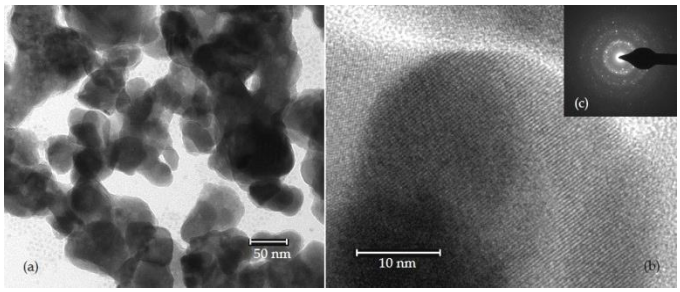


Figure 4: (a)TEM images (b) HRTEM image and (c) SAED image of SBN-50 precursor calcined at 750$^0$C for 6 hours

### 3.4 UV-VIS Optical Study

Since the photorefractive properties of SBN crystals have been studied for optical switch purpose, effect on optical property at nanolevel studied in term of diffuse reflectance spectrum. Fig.5. shows a UV-VIS diffuse reflectance spectrum of SBN50 with reference to the mirror. It is observed the absorption edge is observed at wavelength ~366nm. This value is well matched with the fundamental value of absorption edge reported (370nm) for SBN single crystals [10]. It is also observed that the UV light of wavelengths less than 337 nm are strongly absorbed.

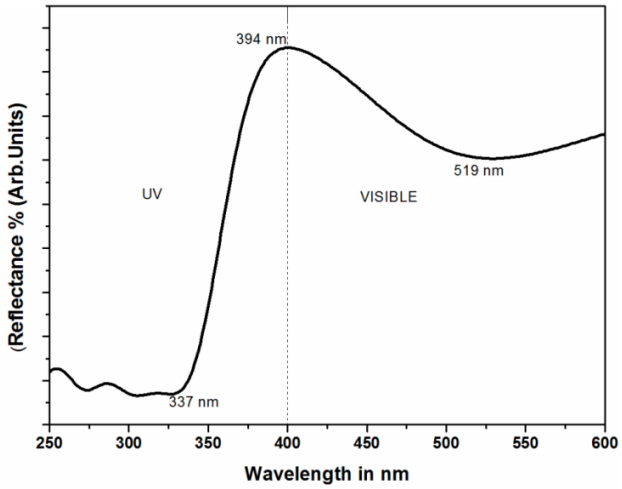


Figure. 5 Diffuse reflectance spectrum of SBN-50 nanoparticles

Fig.6 shows Kubelka-Munk transformed reflectance spectra for as-synthesized SBN50 (Gaussian peak fit data of Fig.5 was used for these graphs). From extrapolation of the linear regions, the optical band gaps are determined [17]. The direct bandgap (n=1/2) and indirect bandgap (n=2) were found to be 3.6 eV and 3.39 eV repectively. The literature reported value of optical bandgap is 3.24eV for SBN-33 single crystal and 3.28eV for SBN61 single crystal [18]. The maximum bandgap value is 3.29eV, which is reported for Cr and Yb codoped SBN58 single crystal [39]. In this regard, the observed bandgap value (for n=1/2) is higher than any individual value of single crystals of SBN. This may be due to nanosized nature of the SBN50.

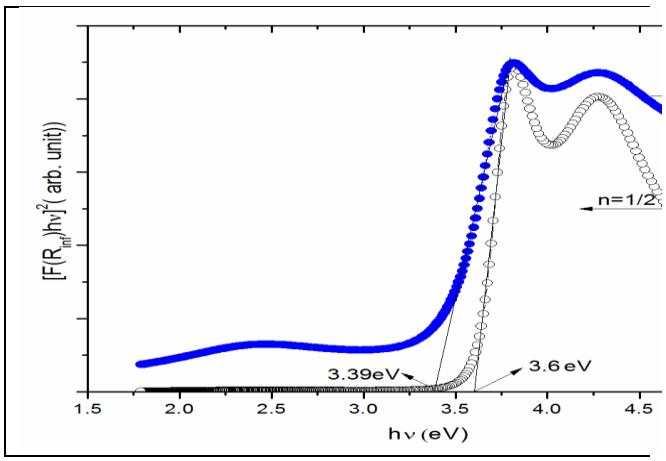


Figure 6 : Kubelka-Munk transformed reflectance spectra of SBN50

## IV. CONCLUSION

SBN-50 nanoparticles of size about 45 nm having better homogeneity and morphology were synthesized by the coprecipitation method. The tetragonal phase of SBN-50 material is observed above 512$^0$C. Low sintering temperature is the key factor for the better morphology and homogeneity. The crystallization was found at 750$^0$C. The weaken hysteresis parameters are due to the size effect of the particles as well as random orientations of the particles. The reflectance spectrum is observed in UV and visible regions. Results obtained are useful to understand the size effect on P 4 b m (space group) material and their related applications.

## V. REFERENCES

[1]. R. R. Neurgaonkar, J. R. Oliver and L.E. Cross, Ferroelectrics (1984) 56, 31-36.

[2]. T. Volk, L. Ivleva, P. Lykov, N. Polozkov, V. Salobutin, R. Pankrath and M. Wöhlecke, Optical Materials (2001) 18 179-182.

[3]. C. David, T. Granzow, A. Tunyagi, M. Wöhlecke, T. Woike, K. Betzler, M. Ulex, M. Imalau and R. Pankrath, Phys. Status Solidi A Appl. Res (2004) 201, R49-R52

[4]. T. Volk, T. Woike, U. Dorfler, R. Pankrath, L. Ivleva and M. Wöhlecke, Ferroelectrics (1997) 203, 457-470.

[5]. M. Oualla , A. Zegzonti , M. Elaatmani, M. Daoud, D. Mezzane, Y. Gagou and P. Saint-Gregoire Ferroelectrics (2003) 291 133-

[6]. S. Podlozhenov, H. A. Graetsch, J. Schneider, M. Ulex, M. Wöhlecke and K. Betzler, Acta Crystallographica (2006) B62, 960-965.

[7]. M. Ulex, R. Pankrath,and K. Betzler, J. Cryst. Growth, (2004) 271, 128-133.

[8]. T. S. Chernaya, T. R. Volk, I. A. Verin, L. I. Ivleva and V. I. Simonov Crystallography Reports (2002) 47, 213-216.

[9]. S. Wanmei, L. Shijun, S. Ranran and W. Chunlong, J. Ceramic Processing Research (2011) 12 716-720.

[10]. S. N. Mathad and V. Puri, Archives of Physics Research, (2013) 3, 106-115.

[11]. S. P. Gaikwad, S. B. Deshpande, Y. Kollam, V. Samual and V. Ravi, Mater Lett. (2004) 58, 3474-6.

[12]. S. R. Dhage, Y. Kollam, S. B. Deshpande and V. Ravi, Mater Res. Bull. (2003) 38, 1601-1605.

[13]. A. V. Murugan, A. B. Gaikwad, V. Samual and V. Ravi, Bull. Mater. Sci. (2006), 29, 221-223.

[14]. F.A. Al-Newaiser, S. A. Al-Thabaiti, A.O. Al-Youbi, A. Y. Obaid and M. A. Gabal, Thermal decomposition kinetics of strontium oxalate, Chem Pap.( 2007) 61, 370-375.

[15]. M. I. Diaz-Guemes, T. Gonzalezcarreno, C.J. Serna, Spectrochim. Acta. A 45 (1989) 589.

[16]. W. Bollmann, H. J. Stohr, Phys. Stat. Sol. A 39 (1977) 477.

[17]. A. E. Morales, E. S. Mora, U. Pal, Rev. Mex. Fis. 53 (2007) 18.

[18]. S. M. Kaczmarek, M. Orowski, T. Skibinski, A. Jasik, L. I. Ivleva, Rev. Adv. Mater.Sci. 23 (2010) 80.

**Cite this article as :**

Sanjay B. Nagdeote, "Structural and UV-Vis Diffuse Reflection Spectroscopy Studies of Nanosized Sr0.5Ba0.5Nb2O6 synthesized by Co-Precipitation method", International Journal of Scientific Research in Science and Technology (IJSRST), Online ISSN : 2395-602X, Print ISSN : 2395-6011, Volume 8 Issue 4, pp. 78-83, September-October 2021. Available at doi : https://doi.org/10.32628/IJSRST218511
Journal URL : https://ijsrst.com/IJSRST218511